Nuclear Engineering and Technology 55 (2023) 3768–3774

Contents lists available at ScienceDirect

Nuclear Engineering and Technology

journal homepage: www.elsevier.com/locate/net

Original Article

RF heating experiment to verify the design process of graphite target at the RAON μSR facility

Jae Young Jeong [a], Jae Chang Kim [a], Kihong Pak [a], Yong Hyun Kim [a], Yong Kyun Kim [a, *], Wonjun Lee [b], Ju Hahn Lee [b], Taek Jin Jang [c]

[a] Department of Nuclear Engineering, Hanyang University, Seoul, 04763, South Korea
[b] Rare Isotope Science Project, Institute for Basic Science (IBS), Daejeon, 34000, Republic of Korea
[c] Department of Physics, Chungang University, Seoul, 06974, Republic of Korea

ARTICLE INFO

Article history:
Received 27 March 2023
Received in revised form
9 June 2023
Accepted 25 June 2023
Available online 27 June 2023

Keywords:
Radio-frequency heating
Muon facility
Muon production target
Surface muon
Graphite target
ANSYS

ABSTRACT

The purpose of the target system for the muon spin rotation, relaxation, and resonance (μSR) facility at the Rare isotope Accelerator complex for ON-line experiments (RAON) is to induce the production of a significant number of surface muons in thermally stable experiments. The manufactured target system was installed at RAON in the Sindong area near Daejeon in 2021. The design was made conservatively with a sufficient margin of safety through ANSYS calculations; however, verification experiments had to be performed on the ANSYS calculations. Because the 600-MeV proton beam has not yet been provided, an alternative way to reproduce the calculation conditions was required. The radio frequency (RF) heating method, which has not yet been applied to the target verification experiment but has several advantages, was used. It was observed that the RF heating method has promise for testing the thermal stability of the target, and whether the target system design process was performed conservatively enough was verified by comparing the RF heating experiments with the ANSYS calculations.

1. Introduction

Graphite targets have been widely studied to generate a variety of particles in accelerator facilities. A typical accelerator facility using a graphite target is a muon production facility, such as the Paul Scherrer Institute/SμS (Switzerland) [1], J-PARC/MUSE (Japan) [2], RCNP/MUSIC (Japan) [3], TRIUMF/CMMS (Canada) [4], and ISIS Neutron and Muon Source (UK) [5]. In addition, China is constructing and planning to build new muon facilities (EMuS) [6]. In South Korea, the Rare Isotope Science Project was launched in December 2011, and a heavy-ion accelerator complex, the Rare isotope Accelerator complex for ON-line experiments (RAON), was designed, including a muon spin rotation, relaxation, and resonance (μSR) facility.

The purpose of the target system for the μSR facility at the RAON is to induce the production of a significant number of surface muons from proton–nucleus interactions in thermally stable experiments. Since muons were discovered by Carl D. Anderson and Seth Neddermeyer at Caltech in 1936 [7], surface muons play an important role in the muon spin rotation, relaxation, and resonance (μSR) techniques. In a prior study, this was achieved by designing a graphite target and target chamber through ANSYS thermal analysis calculations and Monte Carlo particle simulations [8]. The manufactured target system was installed at the RAON in the Sindong area near Daejeon in 2021, and experiments are scheduled to verify whether thermal analysis calculations and surface muon production calculations are performed well.

The μSR facility at RAON will be provided with a 600 MeV proton beam through Super Conducting Linac (SCL) 3 and SCL2 of the RAON Accelerator. Since the construction of SCL3 is not completed, it is not able to proceed with commissioning using a proton beam. The target system was designed conservatively with a sufficient margin of safety through ANSYS thermal analysis calculation; however, verification experiments for ANSYS calculations had to be performed. During operation, heat is generated in the straight-line trajectories of 600-MeV protons passing through the graphite target. To reproduce conditions similar to the actual operating conditions, it is necessary to find a heating method that can reproduce the shape of the heating region so that it is similar to that of the proton beam. In addition, the target rotates in a vacuum

* Corresponding author.
E-mail address: ykkim4@hanyang.ac.kr (Y.K. Kim).

https://doi.org/10.1016/j.net.2023.06.042

during heating. There are a few ways to heat only the desired volume of the graphite target above 1000 °C without contact in a vacuum. The radio frequency (RF) heating method was employed for this purpose [9,10]. The method has not yet been applied to target verification experiments, however, it has several advantages. RF heating is economical and easy to perform. In situations where a beam is not yet available from the accelerator, or when the beam interacts with a target and generates excessively high radiation dose in the surroundings, or in cases where there is significant production of radioactive waste, RF heating can be helpful in verifying the thermal stability of the system. Unlike in experiments using radiation beams, there is no radioisotope production after the experiments, allowing one to examine the thermal damage to the target system. In addition, the heating region can be changed in various ways by altering the shape of the copper coil. In this study, it was found that the RF heating method is promising for testing the thermal stability of the target, and whether the target system design process was performed conservatively enough was verified by comparing the RF heating experiments with the ANSYS calculations.

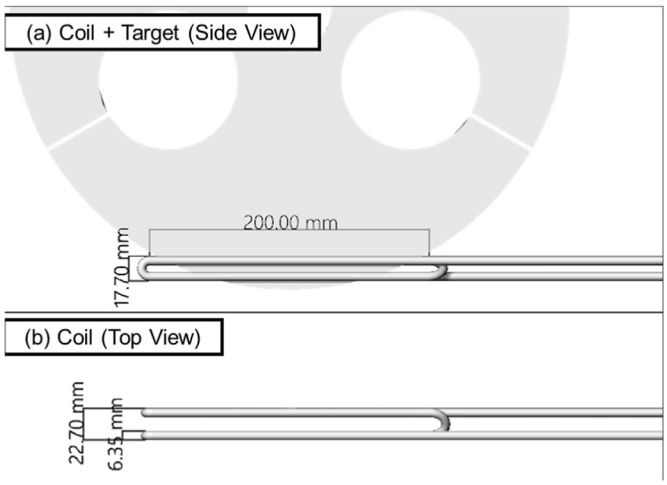

Fig. 1. Copper coil design for the experiment.

2. Configuration

The structure of the μSR target system is described in Section 3.1 of a previous study [8]. The graphite target material was planned to be IG-430U (TOYOTANSO Co., Ltd.), however, it was changed to ET-15 (SHIN SUNG CARBON), which has material properties similar to those of IG-430U and could be supplied faster because it is produced in Korea. The material properties of IG-430U and ET-15 are listed in Table 1. ET-15 has a lower tensile strength than IG-430U; however, it has a lower coefficient of thermal expansion and higher thermal conductivity. This indicates that ET-15 has better thermal stability than IG-430U at high temperatures.

An RF heating machine and copper coil are the most important equipment for performing experiments. The full width at half maximum values of the proton beam in the *X*- and *Y*-directions are 2.7 and 6.75 mm, respectively, at the target position. The copper coil shown in Fig. 1 was designed to cover the beam size and reproduce the heat generated by the beam. The copper coil was connected to the RF heating machine, which could generate an input power of as much as 10 kW. The input power of the device was determined by adjusting the electric current. As the current increases, the voltage gradually increases, and the product of the two values shows the applied input power. The frequency has a value of 10–400 kHz depending on the state of the target. The monitor on the front panel of the RF heating machine shows the electric voltage, current, and frequency. Owing to the performance of the machine, the current is displayed in single digits only. Before the experiments, preheating was performed to reduce the outgassing of the target and copper coil during the experiments. Considering that the magnetic field generated by the AC affects thermocouples, a thermal IR imaging camera (IR camera) is also necessary. A forward-looking infrared (FLIR) SC660 IR camera was used that can measure the temperature range from −40 °C to 1500 °C with a maximum error of 2%. The IR camera measured the temperature of the graphite target through a window from outside the chamber during the heating experiment. Therefore, to observe the temperature of the target with an IR camera, a filter window through which IR rays can pass must be attached to the chamber. The FLIR SC660 IR camera is sensitive to wavelengths from 7.5 to 13 μm. A 2-inch germanium (Ge) window was attached to enable IR rays with a 2–15 μm wavelength to transmit to the outside chamber so that a data point could be recorded using an IR camera.

IR rays are attenuated when passing through a Ge window; therefore, it was necessary to calibrate the measured temperature to the real temperature. Weller WE1010 soldering station was used as a heat source, which the built-in thermocouple located at the tip of the soldering iron measures the temperature of the iron with a maximum error of 5 °C and displays it on the monitor. The situation was reproduced by measuring the distance between the target, window, and camera, and a soldering iron was placed at the target location. Subsequently, while raising the temperature of the soldering iron, the temperature at the soldering iron tip was measured using a thermocouple and an IR camera as shown in Fig. 2. The diagram of the experimental calibration setup and results are shown in Figs. 3 and 4, respectively. As shown in Fig. 4, in the absence of a viewport, the thermocouple and IR camera exhibited similar measurements within a maximum deviation of 5%, and it was observed that the accuracy improved with increasing temperature. When the viewport was installed, the IR camera evaluated the temperature approximately 60.13 times lower than the thermocouple. From these results, we obtained a calibration equation to estimate the actual temperature from the temperature measurements obtained by the IR camera.

Fig. 5 shows the inner view of the target chamber, including the copper coil and graphite target. After the target and coil were placed, a Ge window was attached to the beam port facing the

Table 1
Material properties of IG-430U and ET-15.

Product	Bulk Density (g/cm^3)	Tensile Strength (MPa)	Compressive Strength (MPa)	Young's Modulus (GPa)	Coefficient of Thermal Expansion ($10^{-6}/K$)	Thermal Conductivity (W/(m·K))	Electric Conductivity (S•m)
IG-430U (TOYOTANSO, JAPAN)	1.84	56.8	99	10.8	5.2	140	Unknown
ET-15 (SHINSUNG CARBON, KOREA)	1.84	39.2	111.4	Unknown	4.0	150	95238.1

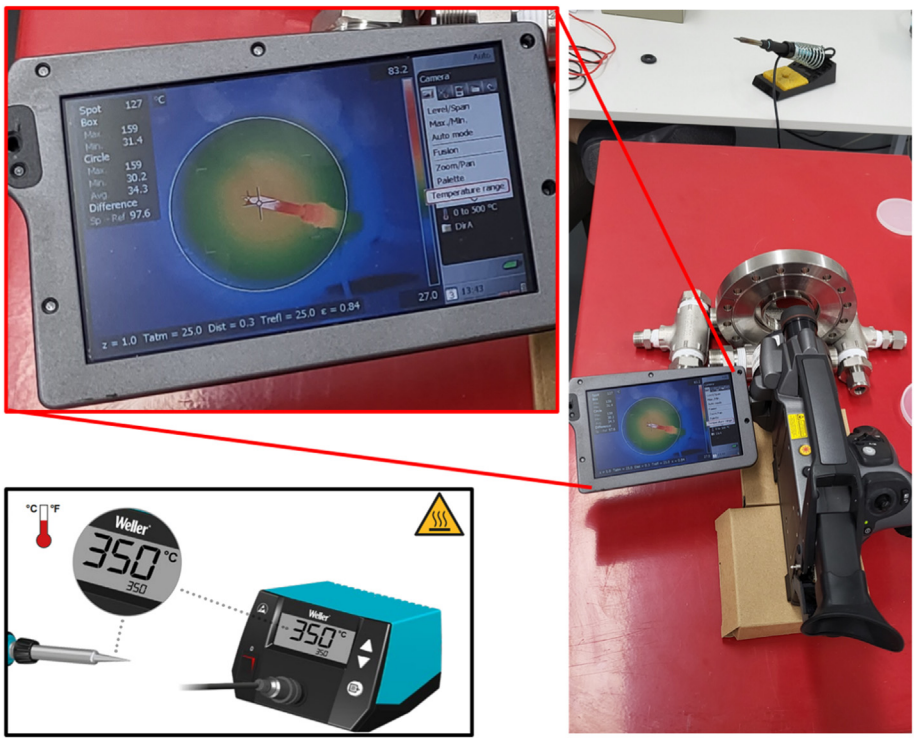

Fig. 2. Temperature measuring using IR camera and Ge window, Screen to monitor the soldering iron's temperature (Top left), Picture showing the part where the thermocouple measures the temperature, indicated in the product manual (Bottom left).

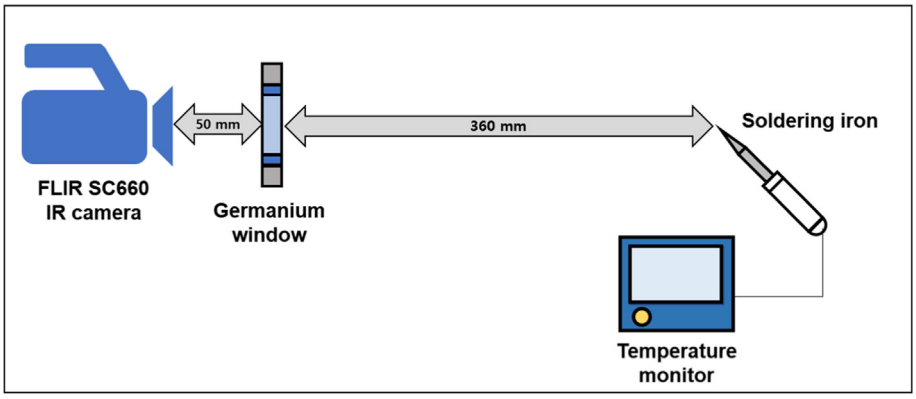

Fig. 3. Diagram of the experimental setup for calibration of temperature measurements through a germanium window.

target. Fig. 6 shows the experimental setup, including the Ge window, IR camera, and target chamber during the experiment.

3. Experiment

The experiment was performed in a stationary state, with the target in a rotational state. The pressure of the target system was kept below 1.333×10^{-4} Pa (10^{-6} Torr) during the experiment.

In the stationary state, the RF heating experiment and ANSYS calculation were compared to verify the design process of the target system. When the target was stationary while heated, the temperature of the target increased partially and not uniformly. Partial heating can cause distortion and breakage of the graphite plate. Accordingly, the input power was increased stepwise, and the maximum temperature was limited to 500 °C. First, the maximum temperature was measured for each input power. In addition, because the current in the machine was only one digit, an excessively low current increased the error in the input power, thus, measuring was started from 5 A.

For the rotating target, the maximum temperature of the target was measured in the same method as for the stationary state. When the target rotated, the generated heat was distributed evenly to the target edges so that a higher input power could be applied than in the stationary experiment. The resonance frequency was 297.5 ± 0.6 kHz for stationary and rotating target states, indicating that tank resonance circuits consisting of the copper coil and the graphite target were almost the same despite the rotation of the target. Furthermore, a rotation experiment was performed to determine the long-term stability of the target system at a high temperature. The highest input power possible was applied, and the target was checked after two weeks to determine whether damage had occurred.

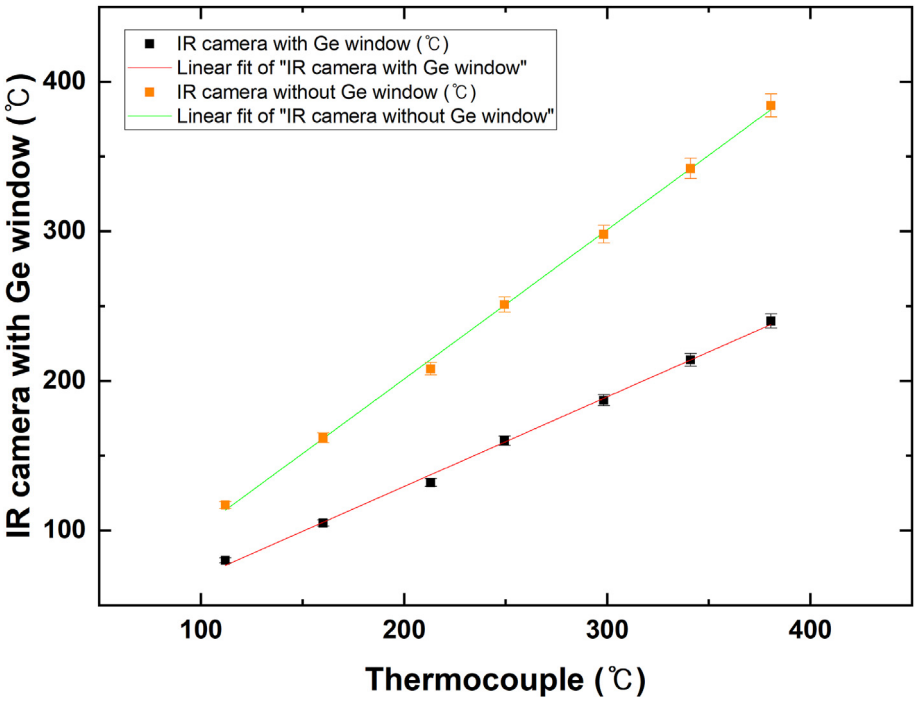

Equation	y = a + b*x	
Plot	IR camera with Ge window	IR camera without Ge window
Weight	No Weighting	
Intercept	9.3648 ± 3.45266	1.77598 ± 3.93442
Slope	0.59986 ± 0.01297	0.99719 ± 0.01478
Residual Sum of Squares	47.24591	61.35057
Pearson's r	0.99883	0.99945
R-Square (COD)	0.99767	0.9989
Adj. R-Square	0.9972	0.99868

Fig. 4. Measurement and calibration result from the experimental setup.

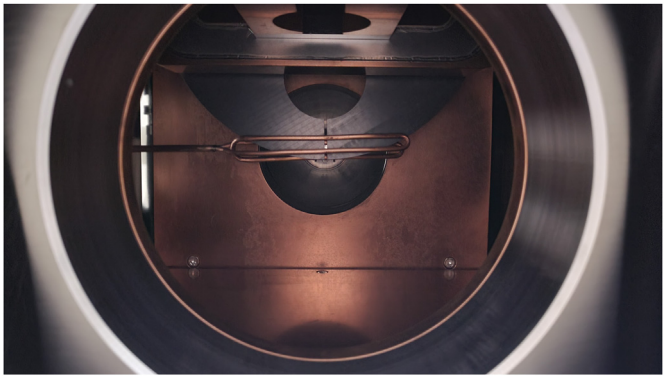

Fig. 5. Inner view of the target chamber showing the copper coil and the graphite target.

4. ANSYS calculation

The ANSYS mechanical package is a powerful tool for calculating the temperature and stress distributions using finite-element analysis solvers. However, some factors can cause uncertainties in the calculation results. Preprocessing for calculation efficiency can cause uncertainty. ANSYS software can import computer-aided design models; however, in many cases, it simplifies the complex parts of the geometry. ANSYS Mechanical requires users to set the radiation heat transfer condition, and the radiation heat transfer was omitted in this study from the detailed parts, such as shafts, the target holder, and bearings. In addition, many materials, including graphite ET-15, have not been studied for their physical properties at high temperatures. Setting thermal conditions, such as convection and radiation at the surfaces, can also result in errors. Therefore, it was necessary to verify that the ANSYS calculation method in the design process can reproduce the experimental results.

Because the ANSYS calculations in the design process were being verified, the ANSYS configuration was similar to that of the design process. However, there were some design changes during the manufacturing process; therefore, the geometry was modified in that area. The thermal properties of copper, SUS304, and Ti–6Al–4V were obtained using the ANSYS Granta Material Database [11]. The material properties for ET-15 were obtained from the SIN SUNG CARBON website. The thermal conductivity reduction of the graphite due to the irradiation was ignored. From the Monte Carlo N-Particle (MCNP) calculation, the average fluence in the designed graphite target was calculated to be 1.555×10^{23} m^{-2} per year. According to previous studies about the neutron irradiation damage to some isotopic graphite product [12,13], that level of neutron fluence is ignorable considering that the lifetime of the graphite target is 28.5 years and the target temperature is above 1200 °C.

In the design step, only the ANSYS mechanical package was applied to the design process, and the amount of heat from the high-energy proton beam collision for each mesh was calculated using MCNP software. However, an additional module, the ANSYS Maxwell package, was applied to the calculation to create RF heat generation. The heat generation rate calculated from the eddy

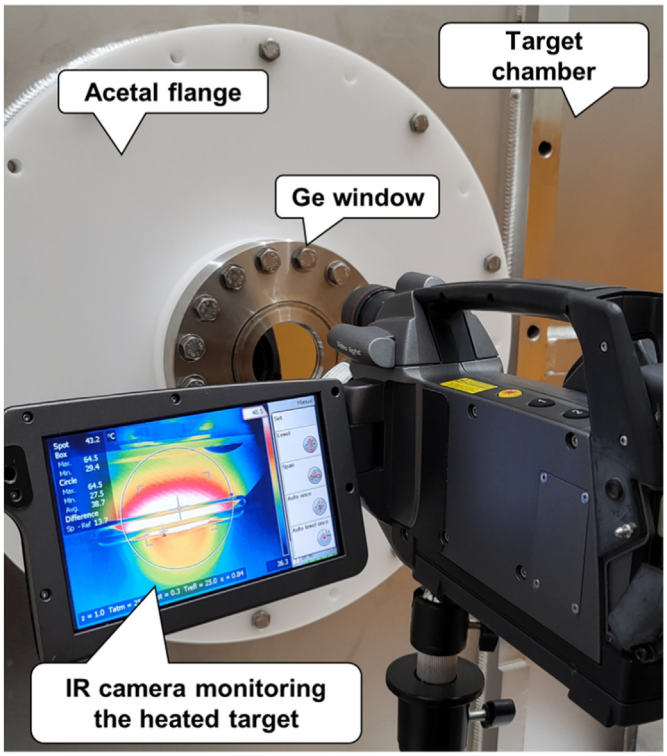

Fig. 6. Experiment setup including Ge window, IR camera, and the target chamber during the experiment.

current solver in the ANSYS Maxwell package can be transferred to the ANSYS Mechanical package using ANSYS Workbench. Thus, the heat generation distribution and amount of heat generated from RF heating can be checked visually. In the ANSYS Maxwell calculation, only the graphite target and copper coil were considered for calculation efficiency. The major input for the ANSYS Maxwell calculation is the amount of current flowing through the coil. However, measuring the current flowing through the coil was challenging due to the extremely high current values. Therefore, we first applied the temperature-dependent electrical conductivity of copper coils and graphite targets to ANSYS Maxwell to calculate the resistance of the inductor. The temperature-dependent electrical conductivity of copper coils and graphite was obtained by the below equation [14].

$$\frac{1}{R} = \frac{1}{R_{ref}\left(1 + \alpha\left(T - T_{ref}\right)\right)},$$

where $R =$ *resistance*,

$R_{ref} =$ *resistance in reference temperature* (*usually* $20^{\circ}C$),

$\alpha =$ *Temperature coefficient of resistance for the material* (0.00393 *for copper*, -0.0005 *for graphite*),

$T =$ *Temperature in degrees Celcius*,

$T_{ref} =$ *Reference temperature that* α *is specified at for the material*

Then, using the power equation, we calculated the current flowing through the coil. Subsequently, we inputted this current back into ANSYS Maxwell to calculate the heat generation distribution. The electrical parameters applied in the ANSYS Maxwell calculation are listed in Table 2.

Unlike the experiment with a stationary target, the experiment with a rotating target is difficult to reproduce in ANSYS Maxwell. However, it was possible to calculate the generated heat from RF heating by using the same method with the ANSYS Maxwell calculation for the stationary state. Instead of the ANSYS Maxwell calculation, the heat distribution calculated by MCNP was used, and the appropriate correction constants were multiplied such that the total amount of heat was equal to the generated heat by RF heating which was calculated by ANSYS Maxwell. The amount of generated heat from RF heating and RF heating efficiency are shown in Table 3. Due to the temperature elevation of the copper coil, electrical conductivity of the coil decreased so that the RF heating efficiency decreased from 20.98% to 17.75% as the input power increased.

5. Test results

The maximum temperatures of the stationary graphite target are listed in Table 4, and a comparison with the ANSYS calculation results is presented in Table 5. The maximum temperature obtained from the calculations shows good agreement with the experimental results, with an error of approximately 3% when difference calculations are performed using the below equation.

$$Difference\ (\%) = \frac{T_{max,Exp} - T_{max,ANSYS}}{T_{max,Exp} - 22^{\circ}C} \times 100$$

At an input power of 1.096 kW to the stationary target, the calibrated maximum temperature reached 464.01 °C, which is close to the determined upper limit of 500 °C. Accordingly, the input power was not increased further, the target was rotated, and the target was heated gradually. The measured maximum temperatures of the rotating target and the ANSYS calculation results are compared in Fig. 7 with the trend line fitted to the power law with the y-intercept of 22 $^{\circ}C$, considering the ambient temperature. Following the application of a maximum input power of 8.6 kW for two weeks, the vacuum on the chamber was released, and the target was visually inspected, confirming that there were no breaks or cracks. The rest of the target system had no problems that were considered in advance, such as the shaft sticking owing to thermal expansion and coolant leaks.

6. Discussion

Although the target was rotating, the graphite target was heated successfully by RF heating, following the power laws, and no thermal damage was observed after two weeks of heating with the maximum input power, as expected. These results show that the RF heating method can be a viable option for heating a rotating graphite target in a vacuum. The input power seems to be too low to check the thermal stability during operation with a 100-kW proton beam. In a previous study, the amount of heat generated from a 100-kW proton beam was believed to be approximately 9 kW. According to Table 5, the RF heating efficiency of the experimental setup was only 20.98% for our target system when the copper coil is well cooled. This result means that it is necessary to prepare an RF heating machine with approximately 5 times higher power to generate a certain amount of heat. From this RF heating efficiency, an input power higher than 50 kW is needed to reproduce the heat generation from a 100-kW proton beam. Because already commercialized RF heating machines have a higher input power of as much as 200 kW, future RF heating experiments are expected to confirm the thermal stability during 100-kW operation.

Table 2
Electrical parameters for ANSYS Maxwell calculation.

Target status	Input voltage (V)	Input current (A)	Input power (kW)	Current flowing through coil (A)	Frequency (kHz)
Stationary	94	5	0.470	159.77	297.5 ± 0.6
	116	7	0.812	206.55	
	137	8	1.096	235.46	
Rotating	129	7	0.903	222.75	
	151	9	1.359	271.87	
	169	12	2.028	328.75	
	198	15	2.97	395.04	
	230	17	3.91	451.60	
	259	19	4.921	504.40	
	282	21	5.922	552.00	
	305	22	6.71	585.51	
	334	25	8.35	652.07	
	344	25	8.6	660.95	

Table 3
The amount of the generated heat and RF heating efficiency for each input power when the target was rotating.

Input power (kW)	Amount of generated heat (kW)	RF heating efficiency (%)
0.903	180.4159	20.98
1.359	266.5853	20.60
2.028	383.4792	19.86
2.97	544.8899	19.27
3.91	705.1304	18.94
4.921	870.434	18.58
5.922	1032.757	18.31
6.71	1152.503	18.04
8.35	1421.115	17.87
8.6	1453.491	17.75

To verify the design process of the target system with the above results, there are some points to consider when comparing the experimental results to the ANSYS calculation.

When the target is stationary, there is a maximum temperature difference of as much as 3% between the experiment and the ANSYS calculation, and the ANSYS calculation shows higher maximum temperatures than the experiments, except at an input power of 0.470 kW. When the target was rotating, the temperature difference between the experiment and ANSYS calculation is lower than approximately 7% error and the ANSYS shows the higher temperature estimation than experiments. Three hypotheses were suggested to explain the temperature difference. First, the emissivity of the graphite target and copper plates surrounding the target, which can vary slightly depending on the surface condition, may have contributed to the error in the results. To address this problem, a measurement process to determine the exact value after processing the target and the copper plates is necessary. Secondly, the material properties of isotropic graphite can vary slightly depending on the specific product. The provided material properties in Table 1 by the purchasing company are for room temperature conditions, and there is currently no research available on the change of material properties with temperature for the ET-15 product. Therefore, there may be some degree of error in the results due to this lack of information. In order to solve this problem, it is necessary to use graphite products, whose material properties at high temperatures are well known, as a target, or to perform a separate material properties measurement. The third reason could be the simplified heat transfer configuration in the ANSYS calculation. The target system geometry was simplified, and the radiation heat transfers were set from only the major parts of the target system for calculation efficiency. In particular, heat conduction at the bearings and bevel gearbox are difficult to calculate using the finite-element method, as in ANSYS, which may cause a difference in the results.

Although the input power is not high enough to test the target system for 100-kW operation, the good agreement of the ANSYS calculation at low input power shows that the maximum temperature of the target in operation with a 100-kW proton beam should be similar to the temperature predicted during the design process. During the design process, the emissivity measurement of each material on the temperature was not performed. However, considering the general trend that emissivity increases with temperature and taking into account the consistent observation that the ANSYS temperature calculation results are consistently higher than the experimental values, the design of the target system was carried out conservatively.

Table 4
Maximum temperatures of the stationary graphite target from the experiment.

Input voltage (V)	Input current (A)	Input power (kW)	Measured temperature by IR camera (°C)	Calibrated temperature (°C)
94	5	0.470	203 ± 4.06	322.64 ± 6.76
116	7	0.812	247 ± 4.94	395.82 ± 8.23
137	8	1.096	288 ± 5.76	464.01 ± 9.59

Table 5
ANSYS calculation results for the stationary graphite target and comparison with experiments.

Input power (kW)	Total heat generated in the target (kW)	RF heating efficiency (%)	Maximum temperature — ANSYS (°C)	Calibrated maximum temperature — Experiment (°C)	Difference (%)
0.470	0.159	20.60	316.32	322.64	−2.10
0.812	0.274	18.88	407.36	395.82	3.09
1.096	0.370	18.47	474.23	464.01	2.31

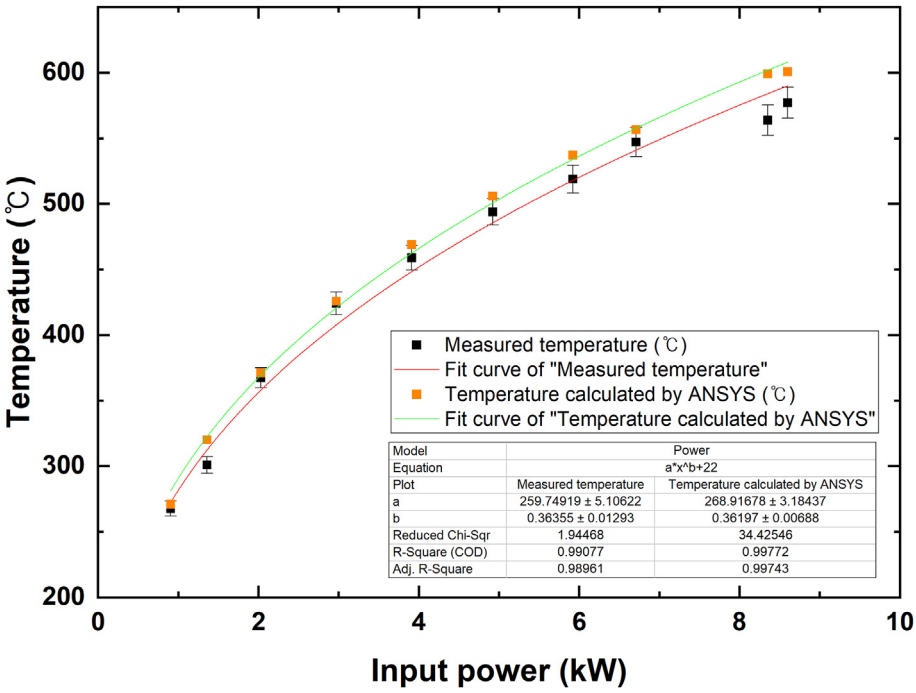

Fig. 7. Maximum temperatures of the rotating target from experiments and ANSYS calculations for each input power and its trend line fitted to the power law.

7. Conclusion

The target system has been installed and is undergoing a pre-operation inspection at RAON in the Sindong area. The target system was designed conservatively with a sufficient margin of safety through the ANSYS thermal analysis calculation; however, verification experiments for ANSYS calculations had to be performed. The RF heating method was thought to be a good option for heating the rotating graphite target in a vacuum, although it had not been applied previously to a target verification experiment. As expected, the graphite target was heated successfully by the RF heating method, and no damage was observed after two weeks of heating at the maximum input power. The results demonstrate that the RF heating method is a viable option to heat the rotating graphite target in a vacuum if sufficient input power is applied. This experiment was limited in that it was only performed with low input power. The μSR facility is planned to operate with a 100-kW proton beam, and the input power in the experiment seems to be considerably low to check the thermal stability during operation with a 100-kW proton beam. However, the consistent overestimation of the ANSYS calculation at a low input power shows that the maximum temperature of the target during operation with a 100-kW proton beam should be lower than the maximum temperature predicted during the design process. Even though there is a limit to the dependence of the material properties on temperature, the comparison between the ANSYS calculation and the experiment indicates that the dependence makes the design process more conservative.

In this study, whether the target system design process was sufficiently conservative with a low input power was examined. If an additional experiment with a higher-power RF machine and a material property analysis of ET-15 graphite is performed, the ANSYS calculation should be closer to the experimental result. As a next step in the verification of the target system design, an experiment to verify the surface muon yield should also be performed with a beam profile monitoring system when a 600-MeV proton beam is used.

Declaration of competing interest

The authors declare that they have no known competing financial interests or personal relationships that could have appeared to influence the work reported in this paper.

Acknowledgement

This work was supported by the Rare Isotope Science Project of the Institute for Basic Science, funded by the Ministry of Science and ICT and the NRF of Korea (2013M7A1A1075764).

References

[1] PSI-LMU: laboratory for muon spin spectroscopy, Available online: https://www.psi.ch/lmu/. (Accessed 15 October 2020).
[2] J-PARC/MUSE, Available online: http://www.j-parc.jp/MatLife/en/index.html.
[3] RCNP–MuSIC, Available online: http://www.rcnp.osaka-u.ac.jp/RCNPhome/music/. (Accessed 1 November 2018).
[4] TRIUMF centre for molecular and materials science, Available online: http://cmms.triumf.ca/. (Accessed 15 October 2020).
[5] ISIS muons, Available online: https://www.isis.stfc.ac.uk/Pages/Muons.aspx. (Accessed 1 November 2018).
[6] J. Tang, X. Ni, X. Ma, et al., Quantum Beam Sci 2 (4) (2018) 23.
[7] C.D. Anderson, S.H. Neddermeyer, Phys. Rev. 50 (1936) 263.
[8] J. Jeong, J. Kim, Y. Kim, et al., Nucl. Eng. Technol. 53 (2021) 2909–2917.
[9] E. Kriezis, T. Tsiboukis, S. Panas, J. Tegopoulos, Eddy currents: theory and applications, in: Proceedings of the IEEE, 80, 1992, pp. 1559–1589, 10.
[10] G. Brown, C. Hoyler, R. Bierwirth, Theory and Application of Radio-Frequency Heating, Van Nostrand, New York, 1947.
[11] Ansys GRANTA EduPack Software, ANSYS, Inc., Cambridge, UK, 2021. www.ansys.com/materials.
[12] A.A. Campbell, Y. Katoh, M.A. Snead, K. Takizawa, Carbon 109 (2016) 860–873.
[13] T. Oku, M. Ishihara, Nucl. Eng. Des. 227 (2) (2003) 209–217.
[14] D.C. Giancoli, Physics, fourth ed., Prentice Hall, 1995.